Structural Engineering and Mechanics, *Vol. 53, No. 1 (2015) 17-26*
DOI: http://dx.doi.org/10.12989/sem.2015.53.1.017

Brazier effect of single- and double-walled elastic tubes under pure bending

Motohiro Sato[*1] and Yuta Ishiwata[2a]

[1]*Faculty of Engineering, Hokkaido University, Kita 13, Nishi 8, Kita-ku, Sapporo 060-8628, Japan*
[2]*Graduate School of Engineering, Hokkaido University, Kita 13, Nishi 8, Kita-ku, Sapporo 060-8628, Japan*

(Received June 12, 2013, Revised March 27, 2014, Accepted April 24, 2014)

Abstract. The cross sections of hollow cylindrical tubes ovalise under a pure bending condition, and this reduces their flexural stiffness as their curvatures increase. It is important to accurately evaluate this phenomenon, known as the 'Brazier effect', to understand the bending behaviour of the systems considered. However, if the tubes are supported by an elastic medium or foundation, the ovalisation displacements of their cross sections may decrease. From this point of view, the purpose of this research is to analytically investigate the bending characteristics of single- and double-walled elastic tubes contacted by an elastic material by considering the Brazier effect. The Brazier moment, which is the maximum moment-carrying capacity of the ovalised cross section, can be calculated by introducing the strain energy per unit length of the tube in terms of the degree of ovalisation for the tube and the curvature. The total strain energy of the double-walled system is the sum of the strain energies of the outer and inner tubes and that of the compliant core. Results are comparatively presented to show the variation in the degree of ovalisation and the Brazier moment for single- and double-walled tubes.

Keywords: elastic tube; pure bending; Brazier effect

1. Introduction

Tube-shaped and thin cylindrical structures are widely used in many engineering fields such as offshore, civil, mechanical, and aircraft engineering. Practical examples range from huge cylindrical tunnel liners (Croll 2001) and pipe-in-pipe systems (Olso and Kyriakides 2003, Kyriakides and Netto 2004, Sato and Patel 2007, Sato *et al*. 2008, Arjomandi, K. and Taheri, F. 2010, 2011a, b, 2012) to very small carbon nanotubes (Ru 2001, He *et al.* 2005, Sato and Shima 2009). These structures are often supported by an inner or outer elastic medium. Analytical investigations of the elastic buckling of a thin cylindrical shell contacted with an elastic material have been conducted for a variety of loading configurations (Yao 1962, Seide 1962, Yabuta 1980, Karam and Gibson 1995, Hutchinson and He 2000, Dawson and Gibson 2007). In the practical design of such structures, one of the most important considerations is the precise estimation of their bending properties.

∗Corresponding author, Associate Professor, E-mail: tayu@eng.hokudai.ac.jp
[a]MSc Student

http://www.techno-press.org/?journal=sem&subpage=8 ISSN: 1225-4568 (Print), 1598-6217 (Online)

Under pure bending, the cross sections of hollow cylindrical tubes ovalise. This reduces the flexural stiffness of the tube as its curvature C increases. The evaluation of this phenomenon, known as the ‘Brazier effect’ (Brazier 1927), is very important to understand the bending behaviour of the systems considered. However, if the tubes are supported by an elastic medium or foundation, the ovalisation displacements of their cross sections may decrease. From this point of view, the purpose of this research is to analytically investigate the mechanisms of the ovalisation phenomena for single- and double-walled tubes supported by an elastic medium by considering the Brazier effect. Results are presented to show the variation in the degree of ovalisation and the Brazier moment with the relative elastic modulus of the filler and tube materials, the filler thickness, and the thicknesses of the inner and outer tubes. The Brazier moment, which is the maximum moment-carrying capacity of the ovalised cross section, can be calculated by introducing the strain energy per unit length of the system in terms of the degree of ovalisation for outer and inner tubes, and the curvature. The total strain energy of the system is the sum of the strain energies of the outer and inner tubes and that of the compliant core. It is also clear that the moment of inertia of the cross section is increased owing to the presence of the core, compared to that of single-walled tubes.

2. Analytical model

Fig. 1 shows the configuration a perfectly cylindrical tube under pure bending. The cross section of the single-walled tube with radius a, thickness t, and Young’s modulus E is assumed to be supported by a Winkler foundation with foundation modulus k, as shown in Fig. 2(a). On the other hand, for the double-walled tube, we consider the Poisson’s effect (Karam and Gibson 1995) of the annulus fully filled with a material (with Young’s modulus E_C and Poisson’s ratio ν_C) that provides continuous structural support to both thin-walled outer and inner tubes with Young’s modulus E_P and Poisson’s ratio ν_P (see Fig. 2(b)). The following are the geometric variables for the double-walled tube: thickness of the outer tube t_1, that of the inner tube t_2, radius of the outer tube a_1, and that of the inner tube a_2. In the following formulation, the subscripts 1 and 2 correspond to the outer and inner tubes, respectively.

As shown in Fig. 3, under pure bending, the cross sections of the hollow, circular cylindrical tube ovalise, thus reducing the flexural stiffness of the tube as its curvature increases.

3. Formulation

3.1 Single-walled tubes on elastic foundation

For the single-walled tube, the strain energies U_θ, U_z, and U_k in the circumferential (θ) and axial (z-) directions and due to the surrounding elastic foundation with the foundation modulus k, respectively, are expressed as follows

$$U_\theta = \frac{1}{2}\int_0^L \int_0^{2\pi} \left[Et\left\{ \frac{v' + w}{a} + \frac{1}{2}\left(\frac{v - w'}{a}\right)^2 \right\}^2 + \frac{Et^3}{12}\left(\frac{v' - w''}{a^2}\right)^2 \right] ad\theta dz \tag{1}$$

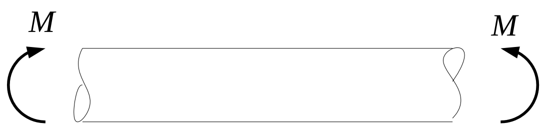

Fig. 1 Elastic tube under pure bending

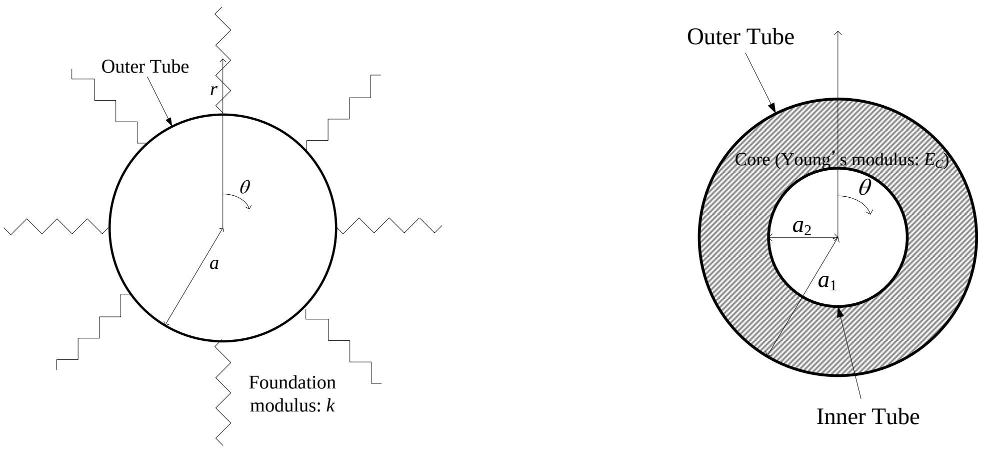

(a) Single-walled tube (b) Double-walled tube

Fig. 2 Cross sections of single- and double-walled elastic tubes

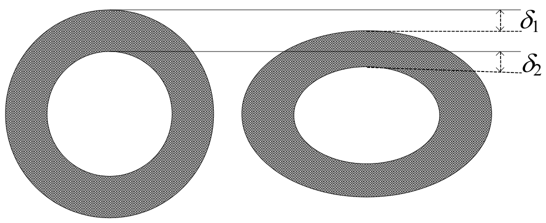

(a) Before bending (b) After bending

Fig. 3 Ovalisation in double-walled tube (the degree of ovalisation is $\zeta_i=\delta_i/a_i$ (i=1, 2))

$$U_z = \frac{1}{2}\int_0^L \int_0^{2\pi} \left[Et\left(u' + \frac{1}{2}w'^2 + \frac{1}{2}v'^2 \right)^2 + \frac{Et^3}{12}w''^2 \right] ad\theta dz \tag{2}$$

$$U_k = \frac{1}{2}\int_0^L \int_0^{2\pi} kw^2 ad\theta dz \tag{3}$$

where (u, v, w) are the deformations of the tube in the axial, circumferential, and radial directions, respectively. Note that the total strain energy $U^{(1)}$ is the sum of the strain energy values obtained from Eqs. (1) to (3). The static equilibrium state under bending can be represented by considering the ovalisation of the cross section, wherein the deformation functions can be derived as follows (Calladine 1983)

$$u = Cz[a\sin\theta + w\sin\theta + v\cos\theta] \tag{4}$$

$$w = a\zeta\cos 2\theta \tag{5}$$

$$v = -\frac{1}{2}a\zeta\sin 2\theta\,. \tag{6}$$

where C is a curvature. The substitution of Eqs. (4)-(6) in Eqs. (1)-(3) and applying the equations of the form

$$\frac{\partial U^{(1)}}{\partial\zeta} = 0 \tag{7}$$

$$M = \int_0^{2\pi} EtC[a\sin\theta + w\sin\theta + v\cos\theta]^2 ad\theta \tag{8}$$

give the non-dimensional parameter ζ of the flattening of the cross section and the corresponding bending moment M.

3.2 Double-walled tube with elastic core

3.2.1 Strain energy associated with ovalisation of core

Here, we develop the formulation for the double-walled tube with elastic core under bending using the procedure proposed by Karam and Gibson (1995). The strain energy U_C per unit length in the ovalised core is expressed as

$$U_C = \frac{1}{2}\int_0^{2\pi}\int_{a_2}^{a_1}(\sigma_r\varepsilon_r + \sigma_\theta\varepsilon_\theta + \tau_{r\theta}\gamma_{r\theta})rdrd\theta \tag{9}$$

where σ_r, σ_θ, $\tau_{r\theta}$ and ε_r, ε_θ, $\gamma_{r\theta}$ are the core stresses and strains in the radial, circumferential, and shear directions, respectively. As shown in Fig. 2(b), the radial and tangential displacement u_i and v_i (i=1 (for outer tube), 2, (for inner tube)), respectively, of the outer and inner pipes ovalised by ζ_i (Calladine 1983) are

$$u_i = a_i\varsigma_i\cos 2\theta = \delta_i\cos 2\theta \tag{10}$$

$$v_i = -\frac{1}{2}a_i\varsigma_i\sin 2\theta = -\frac{1}{2}\delta_i\sin 2\theta \tag{11}$$

The basic equation for the core is expressed by the stress function $\phi\,(r,\theta)$ in polar coordinates (Timoshenko and Goodier 1970) as

$$\left(\frac{\partial^2}{\partial r^2} + \frac{1}{r}\frac{\partial}{\partial r} + \frac{1}{r^2}\frac{\partial^2}{\partial\theta^2}\right)^2\phi(r,\theta) = 0 \tag{12}$$

The normal stresses in the radial and circumferential directions σ_r and σ_θ, respectively, and the shear stress $\tau_{r\theta}$ are determined from

$$\sigma_r = \frac{1}{r}\frac{\partial\phi(r,\theta)}{\partial r} + \frac{1}{r^2}\frac{\partial^2\phi(r,\theta)}{\partial\theta^2} \tag{13}$$

$$\sigma_\theta = \frac{\partial^2 \phi(r,\theta)}{\partial r^2} \tag{14}$$

$$\tau_{r\theta} = -\frac{\partial}{\partial r}\left(\frac{1}{r}\frac{\partial \phi(r,\theta)}{\partial \theta}\right) \tag{15}$$

In the problem considered here, the two displacement components for the core (the radial displacement $u(r,\theta)$ and the circumferential displacement $v(r,\theta)$), are assumed to have circumferentially periodic forms, written as

$$u(r,\theta) = u_C(r)\cos 2\theta \tag{16}$$

$$v(r,\theta) = v_C(r)\sin 2\theta \tag{17}$$

Therefore, $\phi(r,\theta)$ should be expressed as follows

$$\phi(r,\theta) = f_C(r)\cos 2\theta \tag{18}$$

The general solution of Eq. (12) is as follows

$$f_C(r) = \bar{A}r^{-2} + \bar{B} + \bar{C}r^4 + \bar{D}r^2 \tag{19}$$

where $\bar{A}, \bar{B}, \bar{C}$ and $\bar{D}$ are arbitrary constants. In this case, the corresponding stress components are

$$\sigma_r = -(6\bar{A}r^{-4} + 4\bar{B}r^{-2} + 2\bar{D})\cos 2\theta \tag{20}$$

$$\sigma_\theta = (6\bar{A}r^{-4} + 12\bar{C}r^2 + 2\bar{D})\cos 2\theta \tag{21}$$

$$\tau_{r\theta} = (-6\bar{A}r^{-4} - 2\bar{B}r^{-2} + 6\bar{C}r^2 + 2\bar{D})\sin 2\theta \tag{22}$$

The strain components for the plane strain problem are derived by

$$\begin{Bmatrix} \varepsilon_r \\ \varepsilon_\theta \\ \gamma_{r\theta} \end{Bmatrix} = \frac{1}{E_C}\begin{bmatrix} 1-\nu_C^2 & -\nu_C(1+\nu_C) & 0 \\ -\nu_C(1+\nu_C) & 1-\nu_C^2 & 0 \\ 0 & 0 & 2(1+\nu_C) \end{bmatrix}\begin{Bmatrix} \sigma_r \\ \sigma_\theta \\ \tau_{r\theta} \end{Bmatrix} \tag{23}$$

The corresponding displacements in the radial and circumferential directions $u(r,\theta)$ and $v(r,\theta)$, respectively, can be obtained from Eqs. (20)-(23) and thus, the following displacement-strain relationship is derived as

$$u(r,\theta) = \int \varepsilon_r dr = \frac{1+\nu_C}{E_C}\left\{\frac{2\bar{A}}{r^3} + \frac{4\bar{B}(1-\nu_C)}{r} - 4\nu_C\bar{C}r^3 - 2\bar{D}r\right\}\cos 2\theta + P \tag{24}$$

$$v(r,\theta) = \int (r\varepsilon_\theta - u)d\theta = \frac{1+\nu_C}{E_C}\left\{\frac{2\bar{A}}{r^3} + \frac{2\bar{B}(2\nu_C - 1)}{r} + 2\bar{C}(3-2\nu_C)r^3 + 2\bar{D}r\right\}\sin 2\theta + Q \tag{25}$$

where P and Q are constants of integration. For the problem considered here, the outer and inner pipes are assumed to be perfectly bonded to the core. The middle-surface outer pipe displacements

(u_1, v_1) and inner pipe displacements (u_2, v_2) are assumed to have circumferentially periodic forms written as

$$u(a_i,\theta)=u_i \tag{26}$$

$$v(a_i,\theta)=v_i \tag{27}$$

From Eqs. (2), (10), and (11), we can obtain the constants *A*, *B*, *C*, and *D* as functions of δ_1 and δ_2. This indicates that the strain energy associated with the ovalisation of the core (Eq. (1)) can be expressed by the displacements of the outer and inner tubes. Substituting the constants in the stress and strain equations, we obtain the strain energy, which is a function of δ_1 and δ_2.

In addition, we compute the strain energy U_F of the outer and inner flattening tubes (Calladine 1983) as

$$U_F=\sum_{i=1}^{2}\frac{3}{8}\pi E_P\frac{t_i^3}{a_i\sqrt{1-\nu_P^2}}\zeta_i \tag{28}$$

3.2.2 Strain energy associated with bending of double-walled tube

The strain energy U_B per unit length to bend the double-walled tube of flexural rigidity $(EI)_{DWT}$ to a curvature *C* is

$$U_B=\frac{1}{2}(EI)_{DWT}C^2 \tag{29}$$

where

$$(EI)_{DWT}=E(I_1+I_2)+E_CI_C \tag{30}$$

For a hollow pipe with ovalisation, the moments of inertia (Calladine 1983) are

$$I_i=\pi a_i^3t_i(1-\frac{3}{2}\varsigma_i+\frac{5}{8}\varsigma_i^2) \tag{31}$$

$$I_C=\frac{\pi a_1^4}{4}(1-\frac{3}{2}\varsigma_1+\frac{5}{8}\varsigma_1^2)-\frac{\pi a_2^4}{4}(1-\frac{3}{2}\varsigma_2+\frac{5}{8}\varsigma_2^2) \tag{32}$$

Substituting Eqs. (30)–(32) in Eq.(29) gives

$$U_B=\frac{1}{2}C^2E\pi a_1^3t_1(1+\frac{E_Ca_1}{4E_Pt_1})(1-\frac{3}{2}\varsigma_1+\frac{5}{8}\varsigma_1^2)+\frac{1}{2}C^2E\pi a_2^3t_2(1-\frac{E_Ca_2}{4E_Pt_2})(1-\frac{3}{2}\varsigma_2+\frac{5}{8}\varsigma_2^2) \tag{33}$$

Moreover, the strain energy per unit length associated with the Poisson's ratio to maintain the circular cross section due to bending (Karam and Gibson 1995) is then

$$U_P=\frac{1}{2}\int_{a_2}^{a_1}\int_0^{2\pi}(2\sigma_r\varepsilon_r+\tau_{r\theta}\gamma_{r\theta})rd\theta dr=\frac{\pi}{16}\frac{\nu_C^2(5-2\nu_C)}{(1+\nu_C)(1-2\nu_C)}E_CC^2(a_1^4-a_2^4) \tag{34}$$

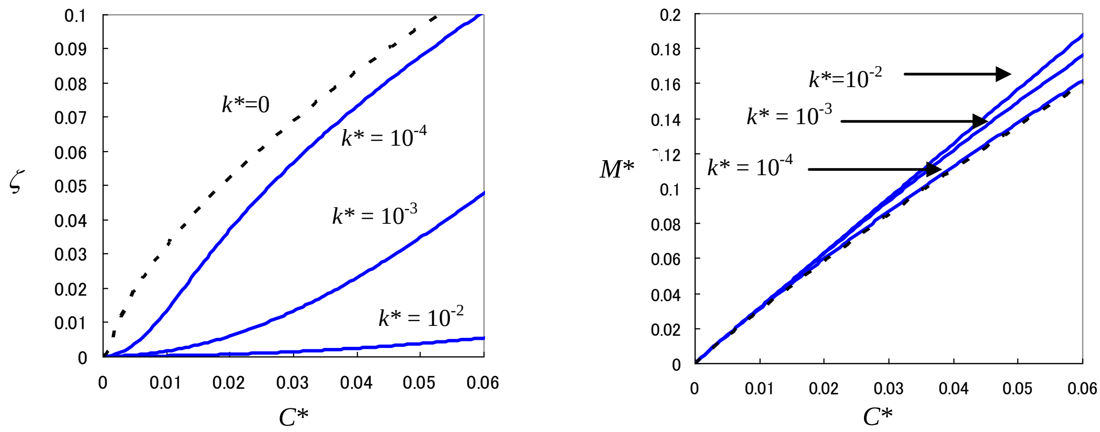

(a) Flattening ratio ζ (b) Non-dimensional bending moment M^*

Fig. 4 Flattening ratio ζ and non-dimensional bending moment $M^*(=M/Eta)$ plotted against the non-dimensional curvature $C^*(=Ca)$ for the single-walled tubes. For both figures, dotted lines correspond to the plots for $k^*=0$

3.2.3 Brazier moment

The final result for the strain energy $U^{(2)}$ of the double-walled system is expressed by the summation

$$U^{(2)} = U_C + U_F + U_B + U_P \tag{35}$$

We can find the optimum values of ζ_1 and ζ_2 for a given value of C from the condition $\partial U^{(2)}/\partial \zeta_i=0$ and thereafter obtain the value for M from $M=\partial U^{(2)}/\partial C$. Moreover, the Brazier moment and ovalisation at the Brazier moment can be obtained from $\partial U^{(2)}/\partial C=0$.

4. Results and discussion

4.1 Single-walled tubes with elastic foundation

Fig. 4 shows the changes in the flattening ratio ζ and the non-dimensional bending moment $M^*(=M/Eta)$ plotted against the non-dimensional curvature $C^*(=Ca)$ for single-walled tubes. It can be seen from Fig. 4(a) that the Brazier effect in tubes with elastic foundation is drastically reduced in the range $k^*>10^{-3}$ by comparing it with the result for tubes with no elastic foundation, i.e., $k^*=0$. However, the rigidity of the surrounding elastic foundation has little effect on the bending moment of the tube. These results provide useful information for the practical structural design of related structures such as buried pipes.

4.2 Double-walled tubes

Figs. 5 (a)-(d) show the plot of the displacement ratio δ_2/δ_1 due to bending against the core thickness ratio a_2/a_1, for various values of the ratio of outer and inner tube thicknesses to the outer tube radius and core-to-tube stiffness ratio. From a comparison of these figures, it is clear that as the core stiffness increases, the displacement of the inner tube increases. Moreover, the effect of the change in the outer tube thickness on the displacement ratio is negligible, and this value can be determined using the core thickness to inner tube thickness ratio.

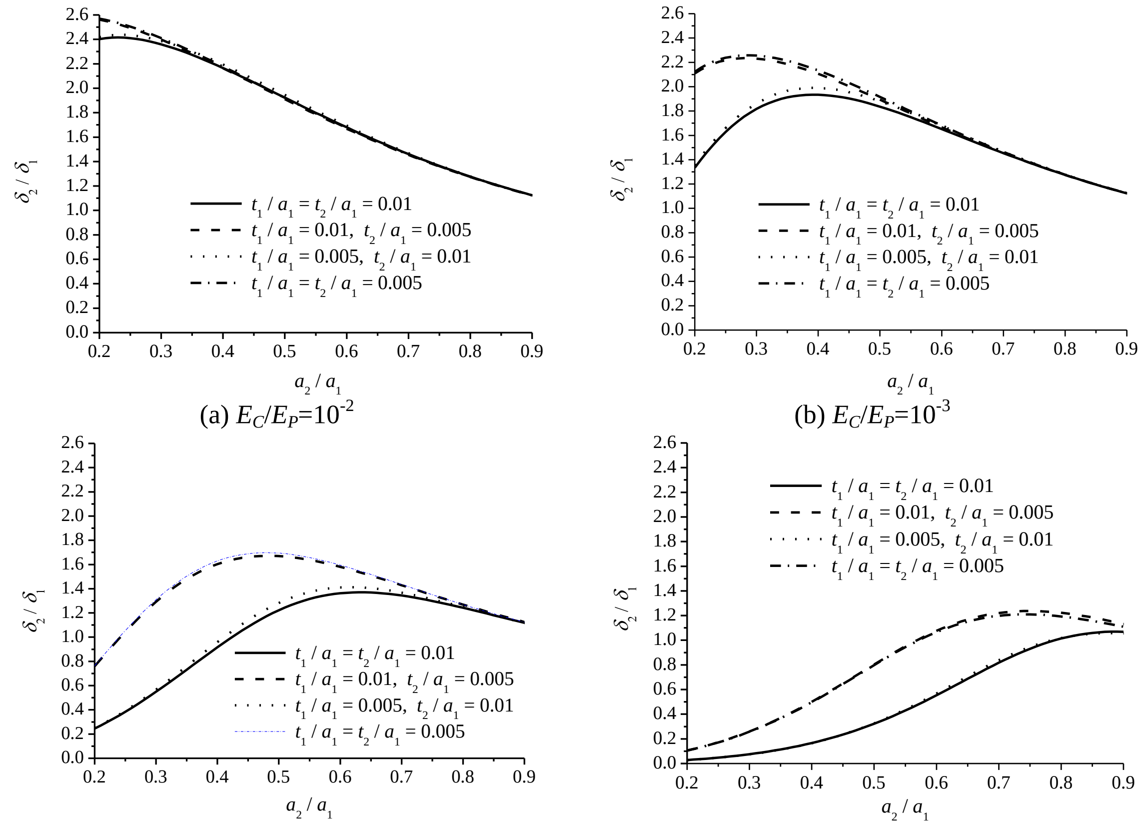

(a) $E_C/E_P=10^{-2}$ (b) $E_C/E_P=10^{-3}$

(c) $E_C/E_P=10^{-4}$ (d) $E_C/E_P=10^{-5}$

Fig. 5 Displacement ratio (Inner to outer pipe, ν_P=0.4)

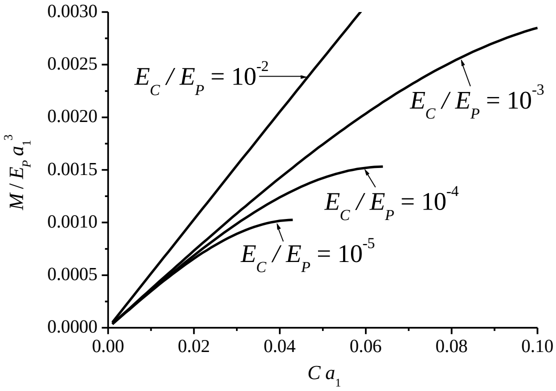

Fig. 6 Non-dimensional moment-curvature relationship (ν_P=0.4, $t_1/a_1=t_2/a_1$=0.01, a_2/a_1=0.5)

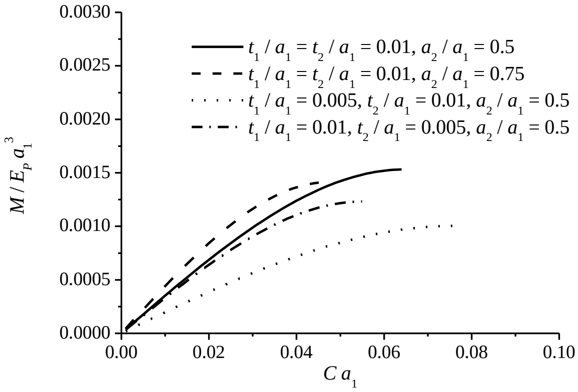

(a) E_C/E_P=10^{-4}

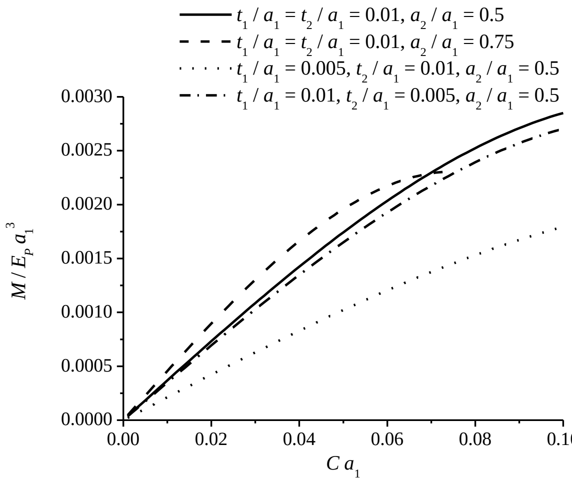

(b) E_C/E_P=10^{-3}

Fig. 7 Non-dimensional moment-curvature relationship (ν_P=0.4)

Fig. 6 and Figs. 7 (a), (b) show the non-dimensional bending moment-curvature relationship. In all cases, for small values of Ca_1, we find that the relationship between the bending moment and curvature is almost linear. However, with increase in curvature increase, the relationship becomes non-linear and finally, the values of M reach the maximum value, i.e., ‘the Brazier moment’. As expected, the Brazier moment increased with increase in core thickness. Figs. 7 (a), (b) show the comparison of the moment-curvature relationship for different outer/inner tube thickness and core thickness ratios. The contribution of the outer pipe thickness is more significant than that of the inner tube to the bending moment-curvature relationship.

5. Conclusions

This paper presents the bending characteristics of single- and double-walled tubes analytically, by considering the Brazier effect. It should be noted that the outer tube thickness and the core stiffness, rather than the inner tube thickness, play an important role in the bending moment-curvature relationship for double-walled tubes. At present, this research is a simplified analytical investigation. However, the author's research group has planned to conduct further studies including the analytical investigations of 'rippling' modes due to buckling under bending.

Acknowledgments

This work was supported by JSPS KAKENHI (Grant no. 24686096).

References

Arjomandi, K. and Taheri, F. (2011), "A new look at the external pressure capacity of sandwich pipes", *Marin. Struct*., **24**(1), 23-42.

Arjomandi, K. and Taheri, F. (2011), "The influence of intra-layer adhesion configuration on the pressure capacity and optimized configuration of sandwich pipes", *Ocean Eng.*, **38**(17-18), 1869-1882.

Arjomandi, K. and Taheri, F. (2011), "Stability and post-buckling response of sandwich pipes under hydrostatic external pressure", *Int. J. Pressure Vessels Pip.*, **88**(4), 138-148.

Arjomandi, K. and Taheri, F. (2012), "Bending capacity of sandwich pipes", *Ocean Eng.*, **48**, 17-31.

Brazier, L.G. (1927), "On the flexure of thin cylindrical shells and other thin sections", *Proceedings of the Royal Society of London* A116, 104-114.

Calladine, C.R. (1983), *Theory of Shell Structures*, Cambridge University Press, Cambridge.

Croll, J.G.A. (2001), "Buckling of cylindrical tunnel liners", *J. Eng. Mech.*, ASCE, **127**(4), 333-341.

Dawson, M.A. and Gibson, L.J. (2007), "Optimization of cylindrical shells with compliant cores", *Int. J. Solids.Struct.*, **44**(3-4), 1145-1160.

Olso, E. and Kyriakides, S. (2003), "Internal ring buckle arrestors for pipe-in-pipe systems", *Int. J. Nonlin. Mech.*, **38**(2), 267-284.

Hutchinson, J.W. and He, M.Y. (2000), "Buckling of cylindrical sandwich shells with metal form cores", *Int. J. Solid. Struct.*, **37**(46-47), 6777-6794.

He, X.Q., Kitipornchai, S. and Liew, K.M. (2005), "Buckling analysis of multi-walled carbon nanotubes: a continuum model accounting for van der Waals interaction", *J. Mech. Phys. Solids.*, **53**, 303-326.

Karam, G.N. and Gibson, L.J. (1995), "Elastic buckling of cylindrical shells with elastic cores - I. analysis". *Int. J. Solid. Struct.*, **32**(8-9), 1259-1283.

Kyriakides, S. and Netto, T.A. (2004), "On the dynamic propagation and arrest of buckles in pipe-in-pipe systems", *Int. J. Solid. Struct.*, **41**(20), 5463-5482.

Sato, M. and Patel, M.H. (2007), "Exact and simplified estimations for elastic buckling pressures of structural pipe-in-pipe cross-sections under external hydrostatic pressure", *J. Mar. Sci. Technol.*, **12**(4), 251-262.

Sato, M., Patel, M.H. and Trarieux, F. (2008), "Static displacement and elastic buckling characteristics of structural pipe-in-pipe cross-sections", *Struct. Eng. Mech.*, **30**(3), 263-278.

Sato, M. and Shima, H. (2009), "Buckling characteristics of multiwalled carbon nanotubesunder external pressure", *Interact. Multis. Mech.*, **2**(2), 209-222.

Yabuta, T. (1980), "Effects of elastic supports on the buckling of circular cylindrical shells under bending", *J. Appl. Mech.*, **47**, 866-870.

Yao, J.C. (1962), "Buckling of axially compressed long cylindrical shells with elastic core", *J. Appl. Mech.*, **29**, 329-334.

CC